Available online at www.sciencedirect.com
ScienceDirect
Journal of Power Sources 175 (2008) 145–158
JOURNAL OF POWER SOURCES
www.elsevier.com/locate/jpowsour

Development of simulated gas diffusion layer of polymer electrolyte fuel cells and evaluation of its structure

Gen Inoue *, Takashi Yoshimoto, Yosuke Matsukuma, Masaki Minemoto

Department of Chemical Engineering, Faculty of Engineering, Kyushu University Motooka, Nishi-ku, Fukuoka 819-0395, Japan

Received 8 May 2007; received in revised form 4 September 2007; accepted 5 September 2007
Available online 14 September 2007

Abstract

In polymer electrolyte fuel cell (PEFC), it is important to understand the behavior of liquid water in gas diffusion layer (GDL) which is one of the constructional elements so as to improve the output performance and the durability. As this behavior of liquid water is attributed to not only the hydrophilicity but also inhomogeneous structure, it is needed to examine in consideration of an actual GDL structure. In this study, as the basic examination of two-phase flow analysis in an actual GDL, a simulated GDL was made by numerical analysis considering the fiber placement. Furthermore, the prediction methods for pore size distribution, permeability and tortuosity of this simulated GDL were developed with the numerical analysis. These parameters of flow and mass transfer were compared with other studies, and the validity of this simulated GDL was confirmed. In addition, effective diffusion coefficient was calculated from tortuosity in simulated GDL, and PEFC output performance was evaluated by a simple model. Moreover, the optimal GDL was examined in consideration of the effect of porosity and fiber diameter at the fiber level.

Keywords: PEFC; Numerical analysis; Gas diffusion layer; Pore distribution; Permeability; Tortuosity

1. Introduction

Recently, global energy consumption increases, and global environmental pollution and destruction of ecosystem turn worse by mass consumption of fossil fuels such as petroleum. The exhaustion of these energy resources becomes a serious problem. In order to solve these problems, the practical application of fuel cells are expected because it emits less environmental pollutant and converts more efficiently from chemical energy to electrical energy than other energy resources. There are various kinds of fuel cells, and polymer electrolyte fuel cell (PEFC) is especially expected as driving power of vehicles and stationary power supply, because it can work at low temperature and has high power density. The performance of PEFC has improved rapidly by developing the new component materials and optimizing the system, and some PEFC systems have already been commercialized. However, in order to spread PEFC for various uses, it is necessary to improve the durability and the cell output, and to reduce the cost. In addition, it is needed to investigate the phenomena which influence the output performance and the durability of PEFC. The power generated by PEFC is affected by the structure, the material and the operating conditions through the process of generation. The phenomena of mass transfer, heat transfer, catalysis, electrochemical reactions and fluid dynamics are shown only in an internal cell, and it is greatly important to understand the correlation among such complex phenomena in detail to improve and optimize the PEFC component and the system.

The phenomena and the mechanism in gas diffusion layer (GDL) which is one of the PEFC components have been studied. The roles of GDL are the followings: the electro transfer between separator and catalyst layer; the mass transfer of hydrogen, oxygen and water between gas channel and catalyst layer; enlarging reaction area of electrode. Accordingly, GDL should be porous media and have high electrical conductivity. In general, GDL is made from carbon materials; carbon paper (non-woven fabric) and carbon cloth. They are distinguished by the difference of the laminated structure of a carbon fiber which is several micrometers in diameter. The improvement of mass transfer rate in GDL is important to generate high power density, and problems of

* Corresponding author. Tel.: +81 92 802 2765; fax: +81 92 802 2785.
E-mail address: ginoue@chem-eng.kyushu-u.ac.jp (G. Inoue).

0378-7753/$ – see front matter © 2007 Elsevier B.V. All rights reserved.
doi:10.1016/j.jpowsour.2007.09.014

Nomenclature

C_m	velocity of virtual particle moving
$C_{O_2}^{channel}$	oxygen concentration at a channel (mol m^{-3})
$C_{O_2}^{e}$	oxygen concentration at an interface of catalyst layer (mol m^{-3})
$C_{O_2}^{ref}$	reference oxygen concentration (mol m^{-3})
d_f	diameter of fiber (m)
D	side length of squared duct (m)
D_m	diffusion coefficient of component m (m^2 s^{-1})
D_{O_2}	oxygen diffusion coefficient (m^2 s^{-1})
D_m^{eff}	effective diffusion coefficient of component m in porous media (m^2 s^{-1})
E	electromotive force (V)
E_m	coefficient in local equilibrium distribution function
f_m	velocity distribution function
f_m^{eq}	local equilibrium distribution function
F	Faraday's constant (C mol^{-1})
i	current density (A m^{-2})
i_{O_2}	exchange current density (A m^{-2})
K	permeability (m^2)
L	length and GDL thickness (m)
m	step number of random walk
n	trial number of random walk
p	pressure in LBM
Δp	differential pressure (Pa)
r	distance of walker from first position (m)
$\langle r^2 \rangle$	mean-square displacement (m^2)
R	gas constant (m^3 Pa mol^{-1} K^{-1})
R_{ohm}	resistance of proton transfer through the electrolyte membrane (Ω m^2)
S_{GDL}	slope of $\Delta p/U$ calculated by LBM with GDL
S_{ref}	slope of $\Delta p/U$ calculated by LBM without GDL
t	time
Δt	time step
T	temperature (K)
$\mathbf{u}$	local velocity in LBM
U	superficial flow velocity (m s^{-1})
V	voltage
x	position
Δx	mesh width
α	parameter of Eq. (11)
α_t	transfer coefficient
γ	variable defined in Eq. (15) (A m mol^{-1})
ε	porosity
ε_p	parameter of Eq. (11)
μ	viscosity (Pa s)
ρ	density in LBM
τ	tortuosity
τ_r	relaxation time
υ	kinematic viscosity in LBM

water management become important in regard to its mass transfer. The proton conductivity of the membrane depends on the moisture content, and the proton conductivity rises as the membrane is wet. Accordingly, supplied gas is usually humidified by humidifier, and the humidity is kept high. It is necessary to maintain the relative humidity in a cell about 100% in order to obtain high output power. However, water condenses when relative humidity exceeds 100% and water droplets appear in GDL and gas channels. The influence of liquid water on cell performance is shown in Fig. 1. When there is liquid water, it prevents reactant gas from diffusing and flowing to electrode, and the mass transfer rate becomes low. As a result, cell voltage drops because of concentration overvoltage. Therefore, it is very important to decrease the bad influences by liquid water and to know the two-phase condition in GDL. Generally, water-repellent GDL is used in order to improve the performance of discharging water. The contact angle of droplet on the surface of GDL is almost more than 90°, and it has hydrophobicity. However, the detailed correlation between the amount of remaining liquid water in GDL and the output performance has not been grasped yet. So the direct observations or measurements of liquid water remaining in GDL have been examined experimentally. In order to measure the two-phase flow condition in GDL which is microscopic and opaque in "in situ" condition, the advanced techniques are required, for example neutron imaging [1–3]. On the other hand, the porous structure and the property of flow and mass transfer in single GDL have been experimentally examined in some studies as a basic evaluation of GDL [4–6]. To put it concretely, the pore distribution, the gas or water permeability and the tortuosity have been evaluated by experiments of flow and mass transfer. As these parameters depend on the kind of GDL structure, the diameter of a carbon fiber, the porosity, the clamp pressure, the PTFE content, these effects have also been examined.

Recently, the internal phenomena are examined by the numerical analysis with the flow and mass transfer property obtained by experiments. The effective diffusion coefficient is calculated by correcting the diffusion coefficient in a free space with porosity, tortuosity and interstitial water saturation. Accordingly, it is needed to measure how much water content is in GDL to know the mass transfer rate of reactant gas (hydrogen or oxygen) from gas channels to catalyst layers. It is so difficult to know this value that some numerical analysis models with two-phase flow condition in GDL have been proposed [7–10]. The interstitial water saturation has been estimated with various operating conditions and current density which affect the rate of water generation and condensation, and the influence of liquid water on the voltage drop have been examined. In our past study, the influence of GDL thickness on current density distribution was examined by numerical analysis [11]. And in [12,13], the mass transfer and the flow in the gas diffusion layers were calculated, and the approximate model for the GDL mass transfer based on the theoretical model was developed. Next, the PEFC reaction and thermal flow analysis model which enabled us to calculate an actual-sized cell was made with this model. The numerical analysis made it possible to examine the separator depth, the GDL effective porosity, the GDL permeability, and the flow rate of

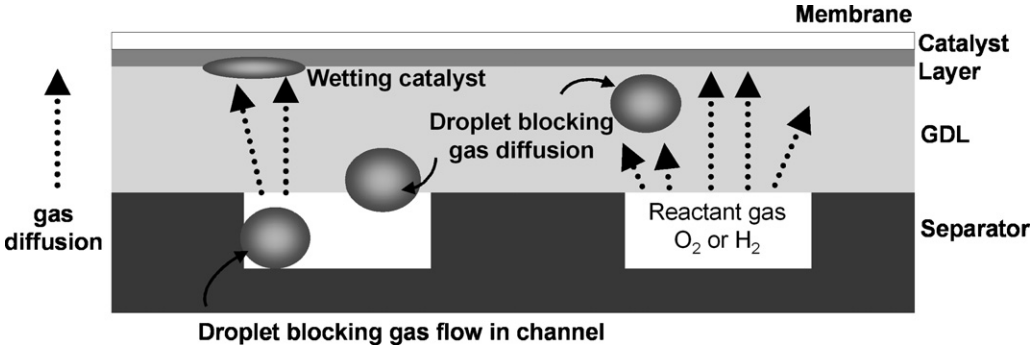

Fig. 1. Influence of liquid water on internal phenomena.

the cathode gas which effected on the output performance and the current density distribution. However, these analysis models simplified the void structure of GDL, and used uniform porosity and permeability. There are few studies which focus on a heterogeneous void structure. We thought that the water permeation in hydrophobic porous media was strongly affected by this heterogeneous structure, and that it was important to examine this heterogeneous structure. In this study, in order to calculate the water permeation in GDL which consists of heterogeneous void structure, as the first stage of the study, simulated GDL was made by numerical analysis considering the fiber placement. And pore size distribution, permeability and tortuosity of this simulated GDL were calculated and compared with other studies. The validity of this structure was examined from the viewpoint of the characteristic of flow and mass transfer on a scale of carbon fiber. In addition, it is thought that these numerical evaluations of the structural property are very important to examine the internal phenomena in GDL and to design GDL structure. Generally, GDL structural properties have been determined by basic experiments, and the data of other references have been often used. In this case, it is not easy to understand the effect of the size of carbon fiber and the lamination in detail. So the effect of the diameter of carbon fiber and the porosity on GDL structural properties was examined by numerical analysis. In addition, effective diffusion coefficient was calculated from tortuosity in simulated GDL, and PEFC output performance was evaluated by a simple model. The results of two-phase flow numerical analysis based on this simulated GDL will be reported in our next paper.

2. Development of simulated gas diffusion layer

2.1. Gas diffusion layer in this study

GDL should be porous media and have high electrical conductivity. In general, GDL consists of fiber materials; carbon paper (non-woven fabric) and carbon cloth. These carbon materials are distinguished by the difference of the laminated structure of the fibers. GDL has water repellent by impregnation of PTFE in order to improve the drainage function. In this study, carbon paper was examined. It is composed of straight carbon fibers dispersed like a plane [14], so the void structure is very complex and not uniform.

2.2. Hypotheses

The simulated GDL was made on the assumptions as follows:

1. Carbon fibers are straight and laid in a plane, and they are not oriented to the direction of GDL thickness.
2. Length of carbon fibers is infinite in the target domain, and fibers do not have cut surfaces.
3. Carbon fibers penetrate mutually when they intersect with each other.
4. The diameter of carbon fibers is uniform and constant in the same GDL.
5. Compression and deformation of fibers by clamp pressure are ignored.
6. Microporous layer (MPL) is ignored.
7. Deformation of a porous structure by water repellent with PTFE is ignored.

Actual carbon fibers in real GDL are not in horizontal planes, and some fibers are oriented to the direction of GDL thickness. However, in this study, it was assumed that the influence of fibers oriented to the direction of GDL thickness on the characteristic of flow and mass transfer was very low and that most of the fibers were set in a two-dimensional plane because of clamp pressure when single cell was assembled. And the development of simulated GDL was simplified. Moreover, the influence of MPL and PTFE content, which are important parts of GDL property, were ignored. These influences will be examined in our next study.

2.3. Development of simulated GDL

On the basis of above assumptions, the simulated GDL was developed by a numerical analysis. The setting parameters were thickness, porosity, diameter of a fiber and degree of orientation, and those values are shown in Table 1. In this study, square area with sides 200 μm was targeted on the horizontal plane, because it was enough to confirm the reproducibility of structural properties, as pore size distribution, which would be explained in the next section. In addition, the simulated GDL with square 400 μm on a side was also made in the base condition shown in Table 1. And the simulated GDL was made three times with each setting parameters, and the reproducibility was confirmed. First, fibers were set horizontally at arbitrary positions and angles in the tar-

Table 1
Setting parameter of development of simulated GDL

Diameter of fiber (μm)	5, 7, 9
Porosity	0.7, 0.6, 0.5
Thickness (μm)	200
Size (μm^2)	200 × 200
Degree of orientation (°)	360

The underlined values are basic condition.

geted domain. The fibers were not cut off in this domain. The position and the angle of fibers were obtained from uniform random numbers. This process was continued until the porosity of one layer became a setting value in each layer. These fiber layers were piled until the GDL thickness became a setting value. By the above-mentioned method, the simulated GDL was made. In this study, the void part and the solid part were set in a cubic lattice 1 μm on a side from the viewpoint of the limits of memory capacity, computational speed and imaging speed. Accordingly, it is necessary to notice that fibers have a ragged surface microscopically. Fig. 2 shows the simulated GDL in a stereoscopic figure and a plane figure in the case of base condition. In this figure, this method numerically developed the porous structure which was similar to real GDL. Fig. 3 shows these structures with each porosity and fiber diameter. In this figure, it was found that the size and the heterogeneity of pore distribution were different from those in other conditions. As stated above, although it was confirmed qualitatively and visually that the simulated GDL was almost same as a real structure observed by a microscope, it was needed to evaluate the porous property and to be compared with that in other studies in order to confirm the validity of the structure. In the next section, the evaluation of the structure was tried.

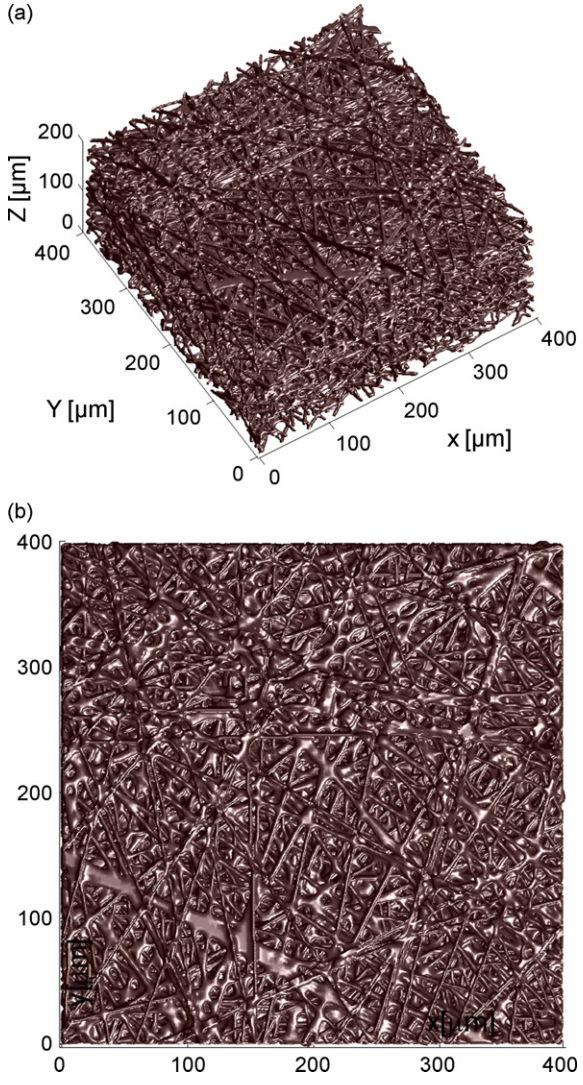

Fig. 2. Structure of simulated GDL developed by numerical analysis in the base condition: (a) stereoscopic figure, (b) plane figure.

3. Evaluation of simulated gas diffusion layer

As it is difficult to compare directly the microscopic void structure of simulated GDL with that of real GDL, macroscopic properties were evaluated. From the point of view of two-phase flow and mass transfer, porosity distribution, surface roughness, pore size distribution, permeability and tortuosity of simulated GDL, which was developed in the previous section, were obtained by the numerical analysis. These results were compared with those of other studies.

3.1. Porosity distribution

In-plane local porosity distribution was examined in order to confirm the reproducibility of simulated GDL. This local porosity was calculated by following method: the average porosity between both GDL surfaces in the direction of thickness was calculated at 1 μm square mesh which was the lattice size in this calculation, and it was obtained at all mesh on GDL surface. Fig. 4 shows the local porosity distribution in the base condition, and Fig. 5 shows the relationship between the statistics of in-plane local porosity and the average porosity with fibers in various diameters. It was found that local porosity was almost homogeneously distributed with a certain degree of error from Fig. 4 and that its statistics became the Gaussian distribution from Fig. 5. So, fibers did not unevenly distribute, and they were dispersed enough. And it was confirmed that the simulated GDL developed in this study was large enough to reproduce the macroscopically averaged structure, and that it was possible to calculate and compare the various structural properties. On the other hand, in Fig. 5, it was found that unevenness of local porosity was reduced by decreasing the fiber diameter. Thus degree of inhomogeneity of average porosity could be evaluated. The other cases showed similar results.

3.2. Surface roughness

Next, surface roughness of simulated GDL was evaluated. It is thought that the surface roughness closely relates to the performance of discharging liquid water in gas channels by hydrodynamical drag of gas flow. In this study, this property was calculated by the local depth from a GDL surface. Fig. 6 shows the local depth distribution in the base condition. In this figure, it was found that some positions are locally deeper owing to the condition of lamination. Fig. 7 shows the relationship

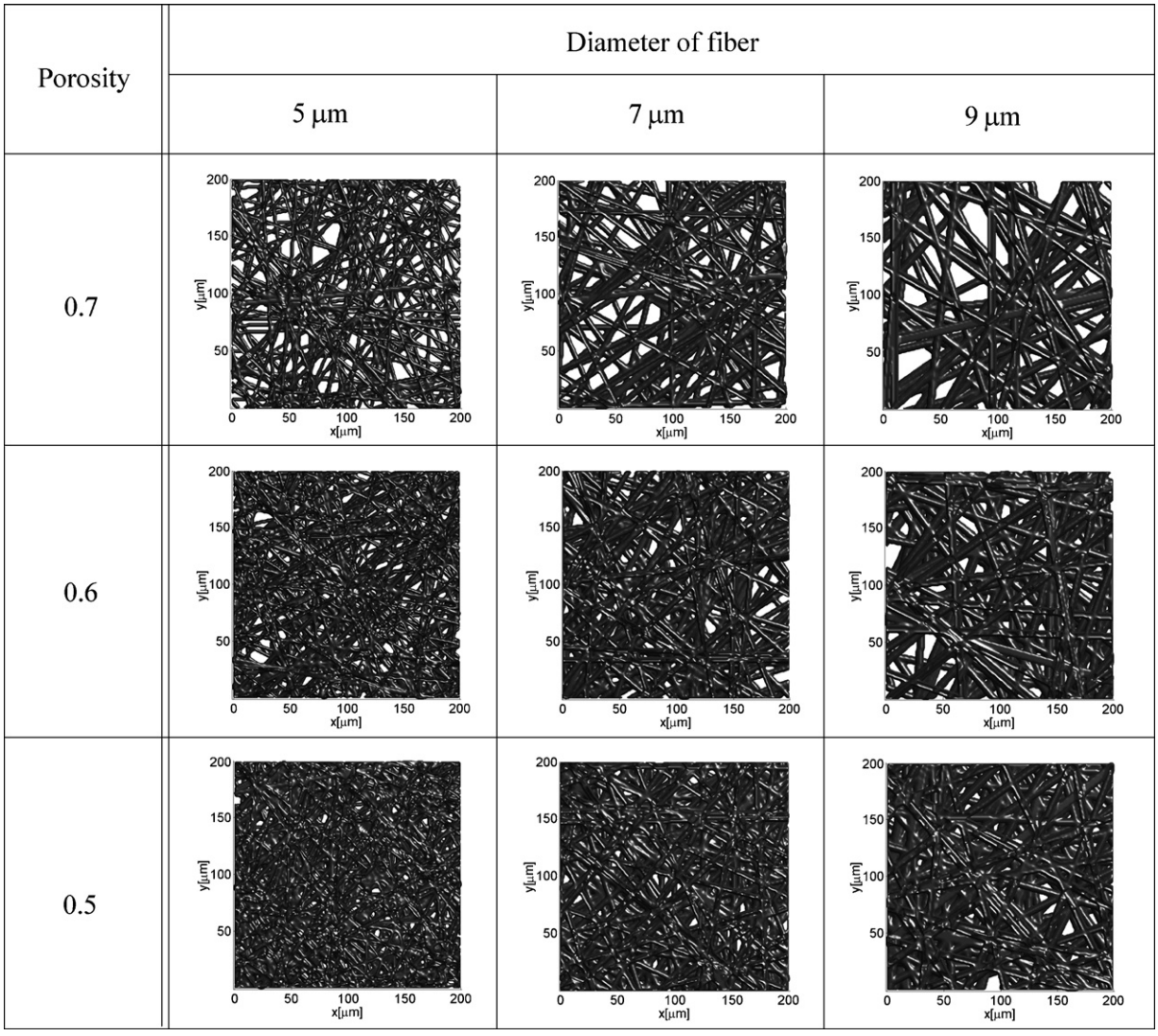

Fig. 3. Structures with each porosity and fiber diameter.

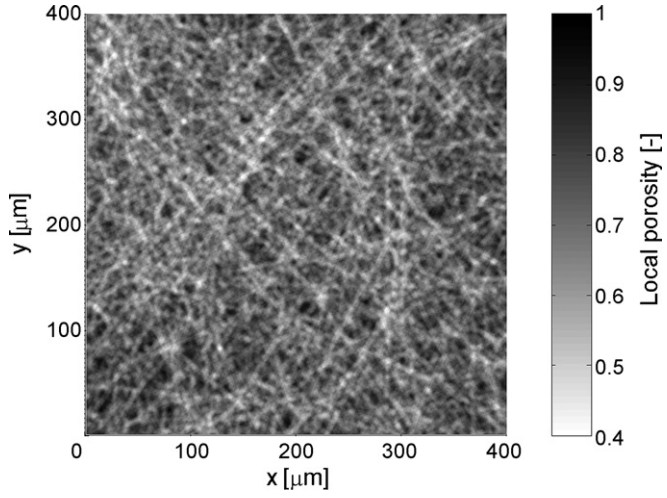

Fig. 4. Local porosity distribution in the base condition; fiber diameter 7 μm, average porosity 0.7, thickness 200 μm.

between the statistics of local depth and the average porosity with fibers in various diameters. In this graph, local depth of a surface was changed by the diameter of a fiber and the average porosity, and the ratio of depth could be expressed by one curve. In addition, it was confirmed that maximum depth was almost equal to thickness of GDL in the case of porosity 0.7, fiber diameter 9 μm, and that some parts between both sides of GDL could directly penetrate. Meanwhile, it is needed to consider the depth of this surface from the other points. The deeper parts become the paths which are straight toward another side for flow and diffusion, and it is thought that such parts are apparently effective in the mass transfer. However, there is liquid water inside GDL when power is generated. Because capillary pressure is very large (capillary number is very small), the transport of liquid water and mass is more strongly affected by local pore size than by the straightness of local path on the basis of facts that capillary pressure is inversely related to pore radius. This pore size distribution is described in the next section, and the two-phase condition in GDL will be examined in the next paper. As there are few other studies about surface

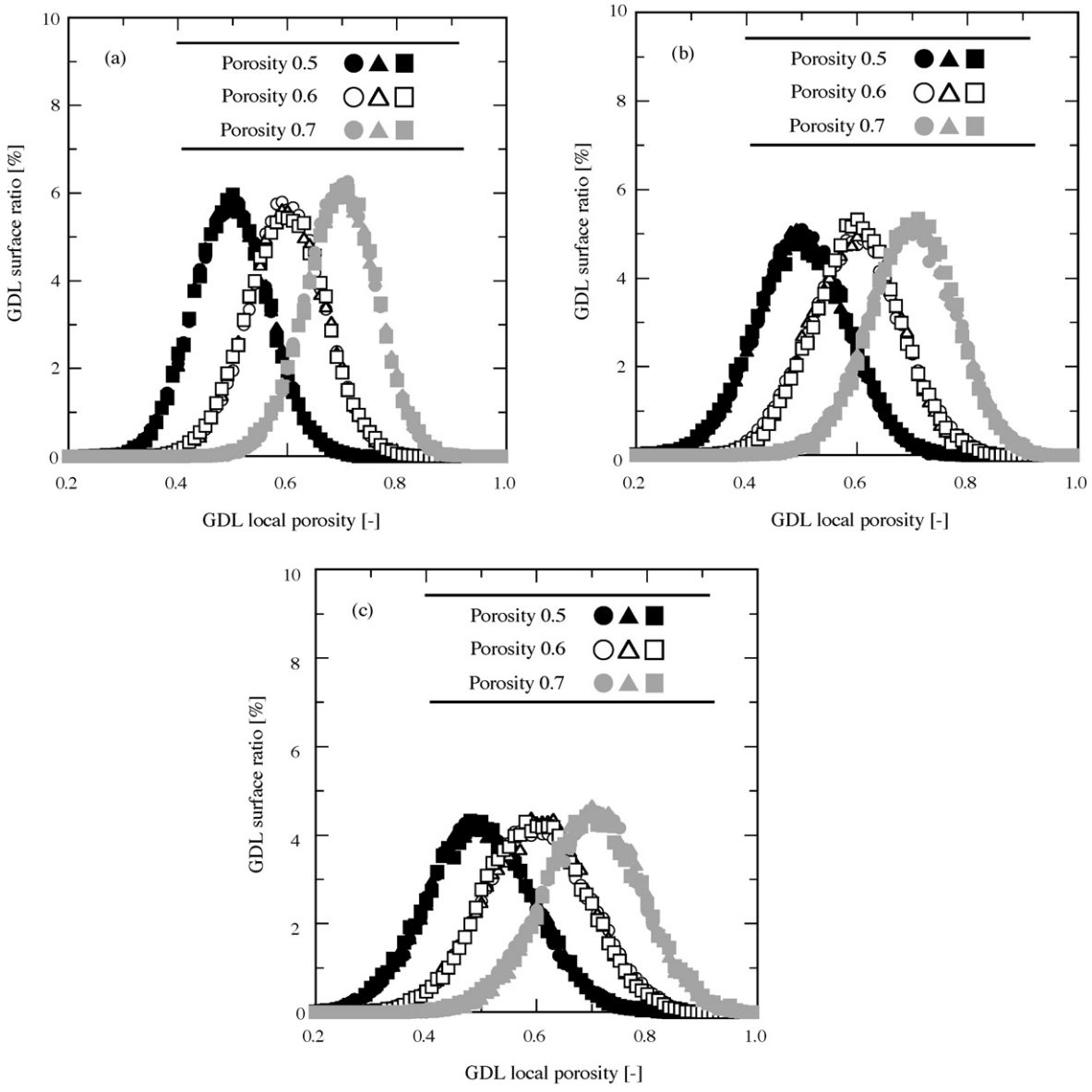

Fig. 5. Relationship between the statistics of in-plane local porosity and the average porosity with three sizes of fiber diameters: (a) 5 μm, (b) 7 μm, (c) 9 μm.

roughness, comparison and verification were not carried out in this study. In our future study, it is needed to confirm the validity by experiments.

3.3. Pore size distribution

The pore size distribution of GDL has been recently discussed in other studies about the structural evaluation and the behavior of two-phase flow, and it is measured experimentally, for example mercury porosimetry. This value is an important factor for structural evaluation and is used to examine the permeation of gas or liquid water. In this study, it was obtained by calculations as follows: the domain which was enclosed with carbon fibers on the plane was extracted, and the area of this domain was obtained; next, the equivalent diameter of the area was calculated, and the calculated value was regarded as a pore diameter. These methods were shown in Fig. 8. In this way, the pore size distribution was obtained by statistics of composition ratio of these pore diameters of all closed domains. Fig. 9 shows the pore distribution of a simulated GDL in various structural conditions. In these graphs, it was confirmed that the structure of the simulated GDL had reproducibility, because the pore distributions of the simulated GDL which were made three times under the same condition almost agreed mutually. The pore size distributions have one peak, and the values were about 10–25 μm. These values were almost equal to actual measurements by the other studies [15,16]. Concerning this result, it has to be noticed that the two-dimensional pore size distribution obtained by void areas in a plane can not be compared simply with the three-dimensional pore size distribution obtained by experiments, because the pore diameter measured by mercury porosimetry with Washburn's equation is affected by the influence of a steric structure. However, it was found that its distribution obtained by this study's method was close to the

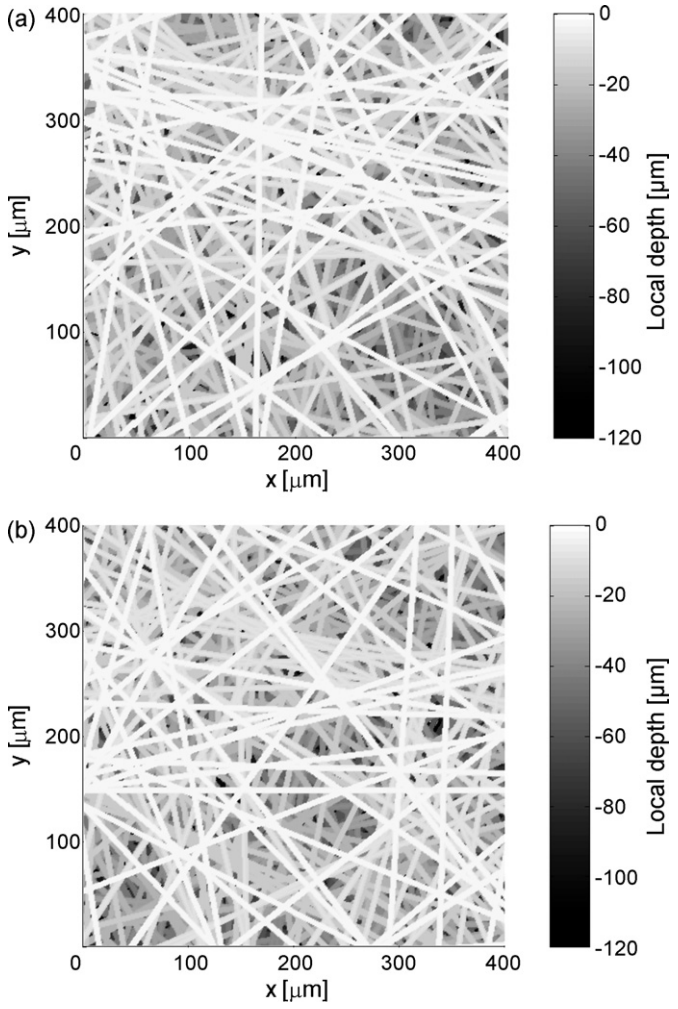

Fig. 6. Local depth distribution in the base condition; fiber diameter 7 μm, average porosity 0.7, thickness 200 μm.

experimental data in the case of anisotropic porous media such as non-woven fabric. In addition, it was found that unevenness of pore was reduced by decreasing the fiber diameter and the average porosity.

3.4. Permeability

Permeability is a parameter of gas flow in porous media, and it has been evaluated as the characteristic of GDL by flow experiments. In this study, the flow analysis in this simulated GDL was carried out by lattice Boltzmann method (LBM), and the permeability was calculated by the relationship between flow rate and differential pressure. LBM is a numerical fluid analysis based on statistical mechanics [17,18]. In this method, it is assumed that continuum fluid is aggregate of numbers of virtual particles which moves only to some definite directions. The collision and the translation of each particle are calculated with the velocity distribution function, and the macroscopic flow field (pressure and velocity) is calculated with the moment of this function. Therefore LBM has analogy with a kinetic theory of gas which treats fluid in the microscopic position. The characteristics of LBM are shown as follows:

- As the collisions and the translations are only repeated, the algorithm is simpler than other methods.
- Unlike a finite differential method and a finite element method, equally spaced mesh is used in LBM, so the grid generation is not needed. In addition, setting a boundary condition of walls simpler, LBM is suitable for calculations in a complex structure.
- Unlike a finite differential method and a finite element method, the calculation is faster because pressure can be explicitly calculated by density.

Moreover, the complex shape of an interface can be calculated, so this method has been applied to a two-phase flow [19–21].

In this study, three-dimensional 15 velocities model (3D15V model), which is shown in Fig. 10, was used as lattice models of LBM. And BGK model was used as the model of collision term. At position x and time t, velocity distribution function $f_m(x,t)$, expresses existing probability of virtual particle moving at a velocity C_m, satisfies the following lattice Boltzmann equation:

$$f_m(x + c_m\Delta x, t + \Delta t) - f_m(x, t) = -\frac{f_m(x, t) - f_m^{\mathrm{eq}}(x, t)}{\tau_{\mathrm{r}}} \tag{1}$$

where f_m^{eq} is the local equilibrium distribution function, τ_{r} the relaxation time, Δx and Δt are the mesh width and the time step, respectively, and these values are one in LBM. In this equation, the left-hand side means the translation of virtual particle, and the right-hand side means the change of velocity distribution function by collisions. The local equilibrium distribution function is calculated by the following equation:

$$f_m^{\mathrm{eq}}(x, t) = E_m\rho\left[1 + 3\mathbf{c}_m \cdot \mathbf{u} + \frac{9}{2}(\mathbf{c}_m \cdot \mathbf{u})^2 - \frac{3}{2}\mathbf{u} \cdot \mathbf{u}\right] \tag{2}$$

where $\mathbf{u}$ is the local velocity, ρ the density. The coefficient E_m is fixed in order to satisfy Navier–Stokes equation and the definitional equation of density and velocity, and these values of 3D15V model are shown in Table 2. Fluid density ρ and flow velocity $\mathbf{u}$, which are macroscopic variable, are defined with velocity distribution function f_m as follows:

$$\rho = \sum_{m=1}^{N} f_m \tag{3}$$

$$\mathbf{u} = \frac{1}{\rho}\sum_{m=1}^{N} \mathbf{c}_m f_m \tag{4}$$

Table 2
Coefficient E_m of 3D15V model

$m = 1$	$E_m = 2/9$
$m = 2$–7	$E_m = 1/9$
$m = 8$–15	$E_m = 1/72$

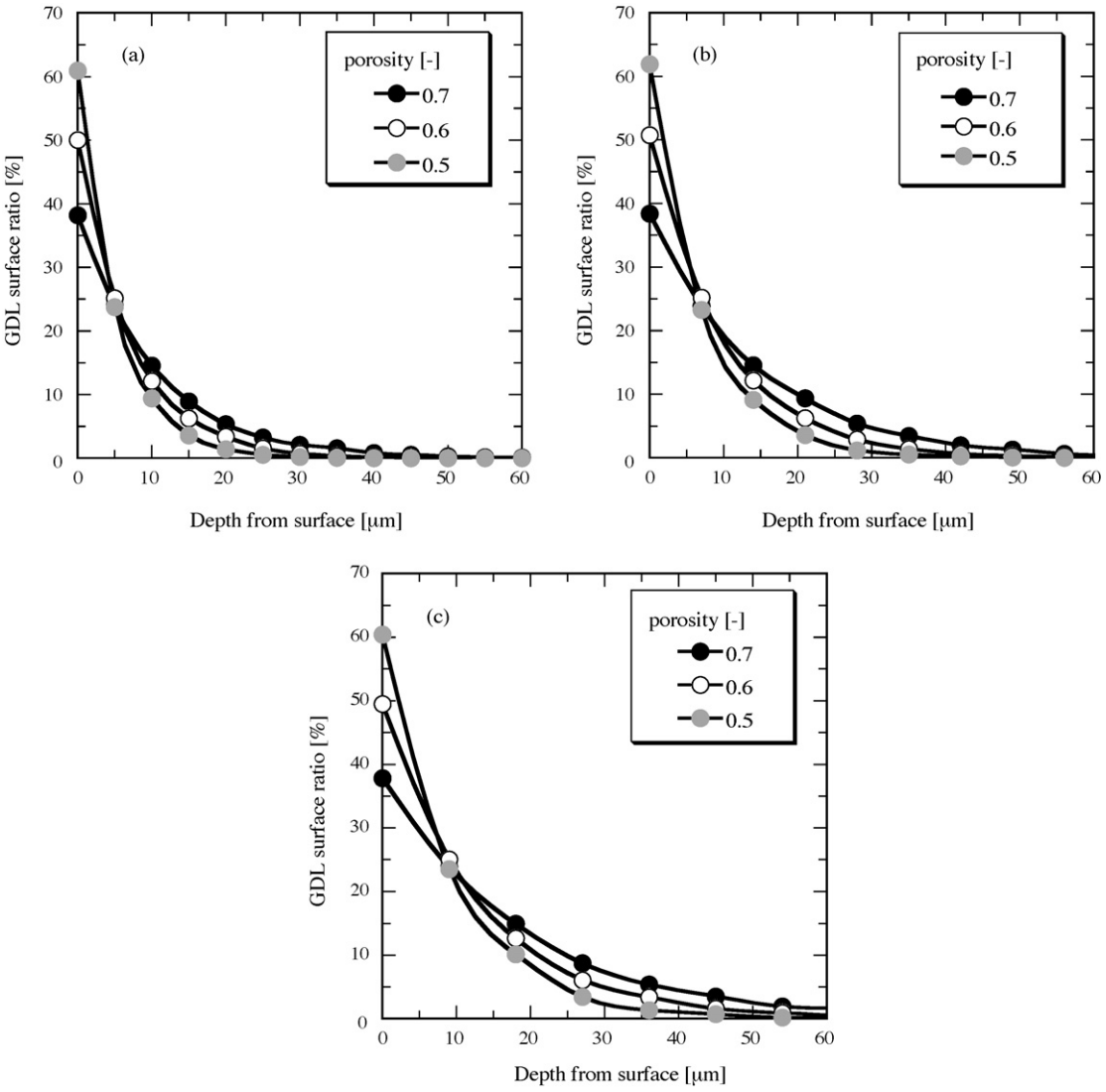

Fig. 7. Relationship between the statistics of local depth and the average porosity with three sizes of fiber diameters: (a) 5 μm, (b) 7 μm, (c) 9 μm.

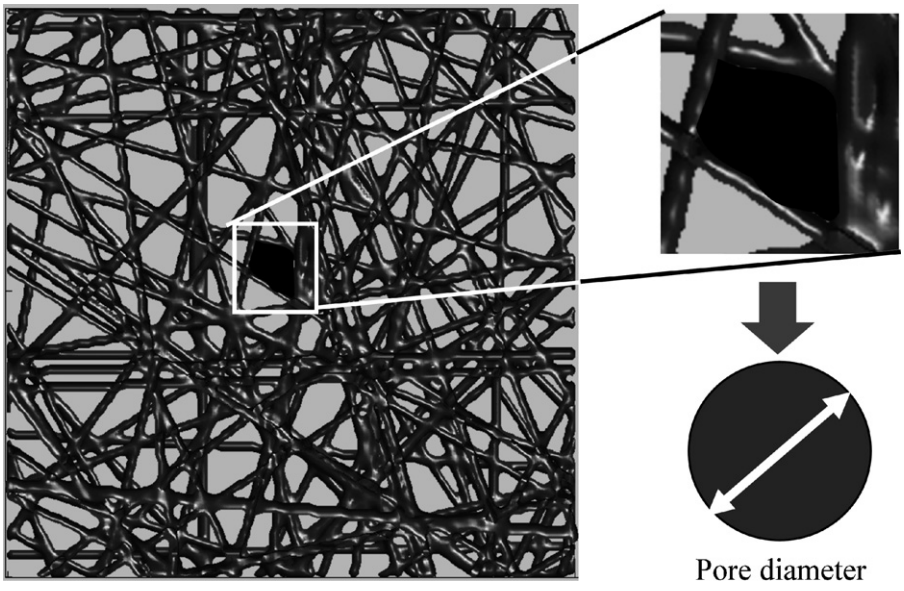

Fig. 8. Schematic diagram of method to obtain pore size distribution.

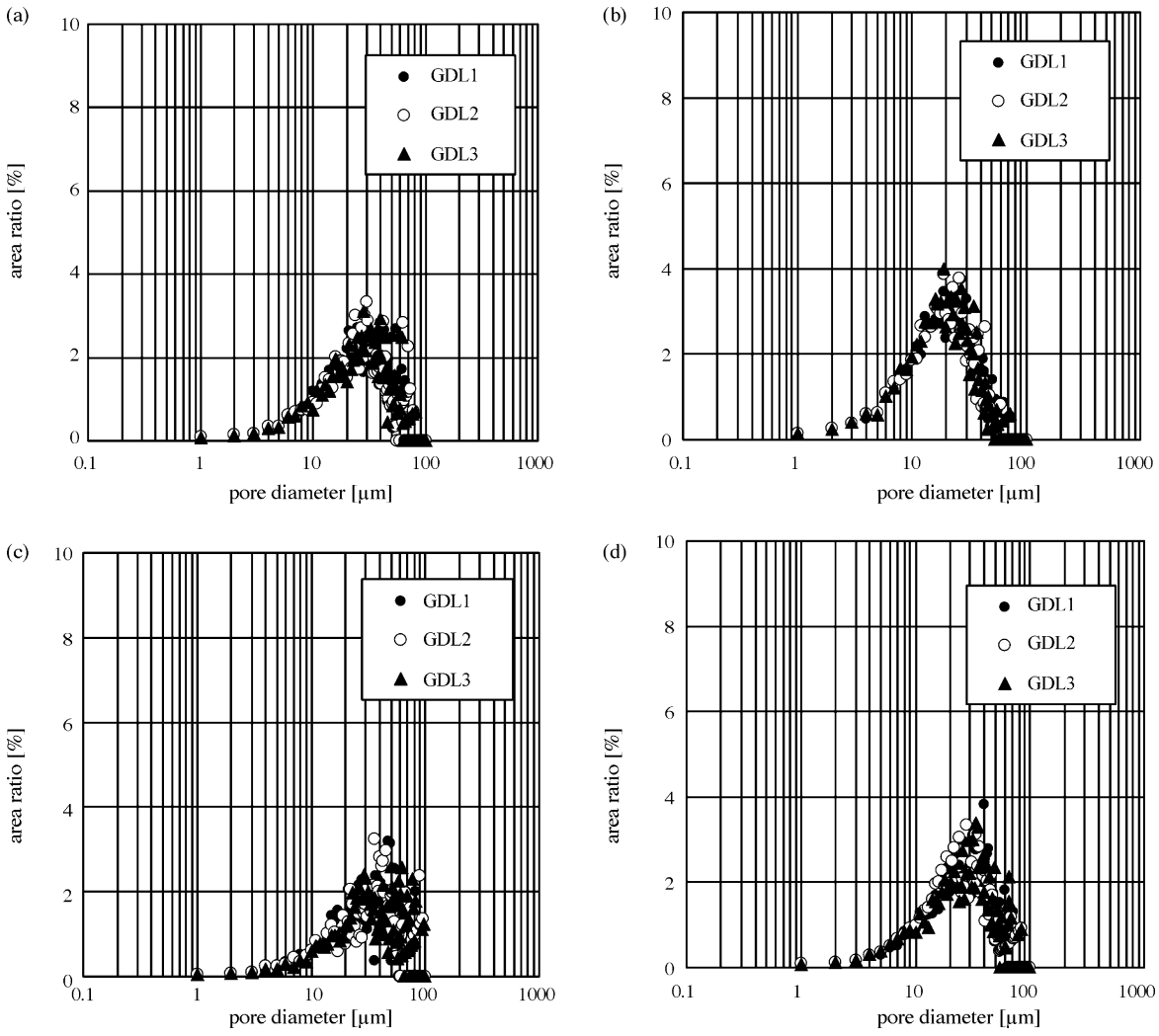

Fig. 9. Pore size distribution of simulated GDL with various sized diameter and porosity of fibers: fiber diameter (a) and (b) 7 μm, (c) and (d) 9 μm; porosity (a) and (c) 0.7, (b) and (d) 0.6.

Pressure p is proportional to density, and it is defined as follows:

$$p = \frac{\rho}{3} \tag{5}$$

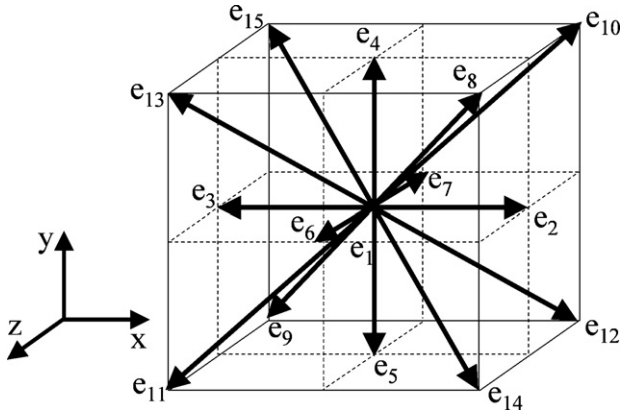

Fig. 10. Lattice structure of three-dimensional 15 velocities model (3D15V model) of LBM.

Kinematic viscosity υ is calculated as the function of relaxation time.

$$\upsilon = \frac{1}{3}\left(\tau_{\mathrm{r}} - \frac{1}{2}\right) \tag{6}$$

As mentioned above, LBM can be applied to direct fluid analysis in porous media with complex structure such as GDL. However, as all variables are dimensionless values in LBM, it is not possible to calculate them with concrete physical quantity. Accordingly, the actual value of pressure drop and permeability cannot be calculated directly. So the permeability of simulated GDL was obtained by the following method in this study. In Fig. 11, simulated GDL was set in a squared duct, and supplied gas flowed from the downside in various superficial flow velocity (U). Then, differential pressure between both sides of GDL (Δp) was obtained by LBM. In calculation by LBM, these differential pressure and flow rate are dimensionless values. Assuming the gas flow in simulated GDL could be approximated by Darcy's law, the slope S_{GDL}, which equalled to $\Delta p/U$, was calculated by a least-squares method. Similarly, the slope S_{ref} was calculated in the case of no GDL, as reference.

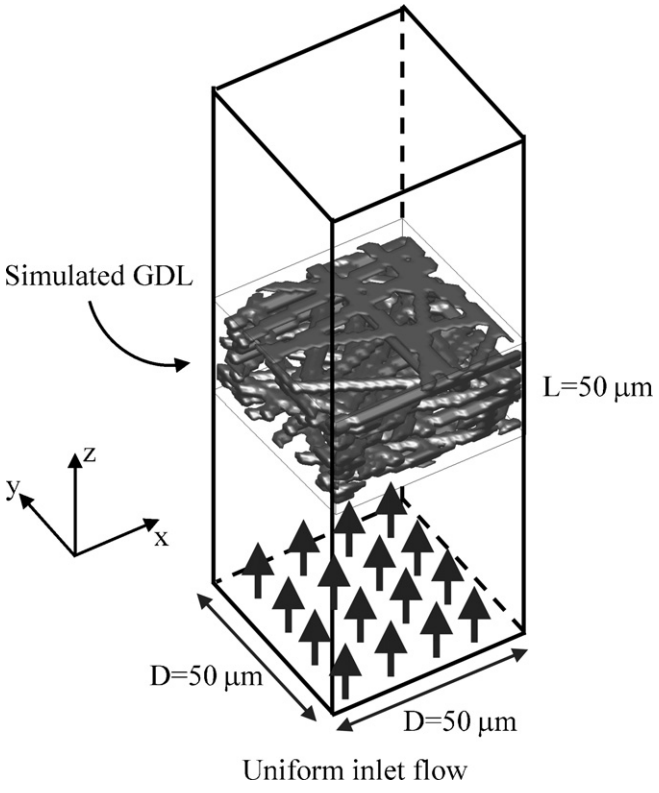

Fig. 11. Calculation model of gas flow in GDL for evaluation of permeability.

On the other hand, the relationship between pressure drop and gas flow velocity in porous media is theoretically calculated by the following Darcy's law [22]:

$$\Delta p = \frac{\mu L}{K} U \tag{7}$$

where K is the permeability, μ the viscosity and L the section length. In addition, the pressure drop in a squared duct without porous media is calculated by the following equation which is derived from Hagen–Poiseuille law and a friction coefficient of the squared duct [23]:

$$\Delta p = \frac{28.44 \mu L}{D^2} U \tag{8}$$

D is the side length of squared duct. Assuming the ratio between S_{GDL} and S_{ref} obtained by LBM was the same that between Eqs. (7) and (8), the following equation was derived:

$$S_{\mathrm{GDL}} : S_{\mathrm{ref}} = \frac{\mu L}{K} : \frac{28.44 \mu L}{D^2} \tag{9}$$

By developing the equation above, the following permeability equation is obtained:

$$K = \frac{D^2}{28.44} \frac{S_{\mathrm{ref}}}{S_{\mathrm{GDL}}} \tag{10}$$

In this study, the in-plane and through-plane permeability of simulated GDL was calculated by the process above, and the relationship between permeability and porosity was calculated with various GDL. Furthermore, this result was compared with that of other studies in order to verify the validity. Gostick et al. [24] measured the in-plane and through-plane permeability of various GDL, and the effect of porosity was examined by compressing. Besides, it was confirmed that these results exactly agreed to the results of the following Tomadakis–Sotirchos model (TS model) which estimated permeability of fibrous porous media [25]:

$$K = \frac{\varepsilon}{32(\ln \varepsilon)^2} \frac{(\varepsilon - \varepsilon_{\mathrm{p}})^{(\alpha+2)} d_{\mathrm{f}}^2}{(1 - \varepsilon_{\mathrm{p}})^{\alpha} [(\alpha + 1)\varepsilon - \varepsilon_{\mathrm{p}}]^2} \tag{11}$$

where d_{f} is the diameter of fiber, ε the porosity, α and ε_{p} are the constants that depend on the structure and on the flow direction. When randomly set fibers form a plane and such planes are parallel to each other, α and ε_{p} are respectively 0.521 and 0.11 in the case of in-plane flow. And in the case of through-plane flow, these values are 0.785 and 0.11, respectively. Fig. 12 shows an example of flow analysis results by LBM in a simulated GDL. In this graph, flow velocity distribution in porous media which is a complicated shape was calculated by this method. These analyses were carried out on other GDL, and the differential pressure and permeability were obtained. Fig. 13 shows the calculation results and TS model standing for a relationship between in-plane and through-plane permeability and porosity in the case of fiber diameter 5 μm and 9 μm. In these graphs, it was found that the calculation results were almost equivalent to TS model in the case of in-plane flow, and that validity could be confirmed. So, this calculation method was effective to predict permeability. However, the calculation results of through-plane permeability were different from results obtained from a model equation; the former was twice as much as the latter. And the permeability in both directions was almost equal to each other. Though the permeability of an actual non-woven fabric has anisotropy, it was thought that this difference arose owing to the insufficiency of calculating area and low-resolution mesh in this study. Nonetheless the approximate permeability equivalent to model equations could be predicted by this analysis method though it had a certain amount of error.

3.5. Tortuosity

Tortuosity is an important parameter of mass transfer in porous media. The effective diffusion coefficient in porous media with porosity and tortuosity is shown as follows:

$$D_m^{\mathrm{eff}} = D_m \frac{\varepsilon}{\tau} \tag{12}$$

Generally, tortuosity of isotropic porous media, such as spherical particle, is obtained by Bruggeman equation [26]. However, this equation cannot be used in the case of non-woven fabric because of its anisotropic structure. Tomadakis and Sotirchos calculated tortuosity of fibrous porous media and modeled its equation by random walk method [27]. In this study, the validity of tortuosity in simulated GDL was confirmed by random walk method. In the calculation by Tomadakis and Sotirchos, tortuosity was obtained when the overall direction of mass transfer was given previously. In this study, as a supplementary examination, tortuosity was calculated in the case that the mass transfer direction was not given by the method of Watanabe and Nakashima [28]. In simulated GDL, walker takes a step of lattice size to the arbitrary direction

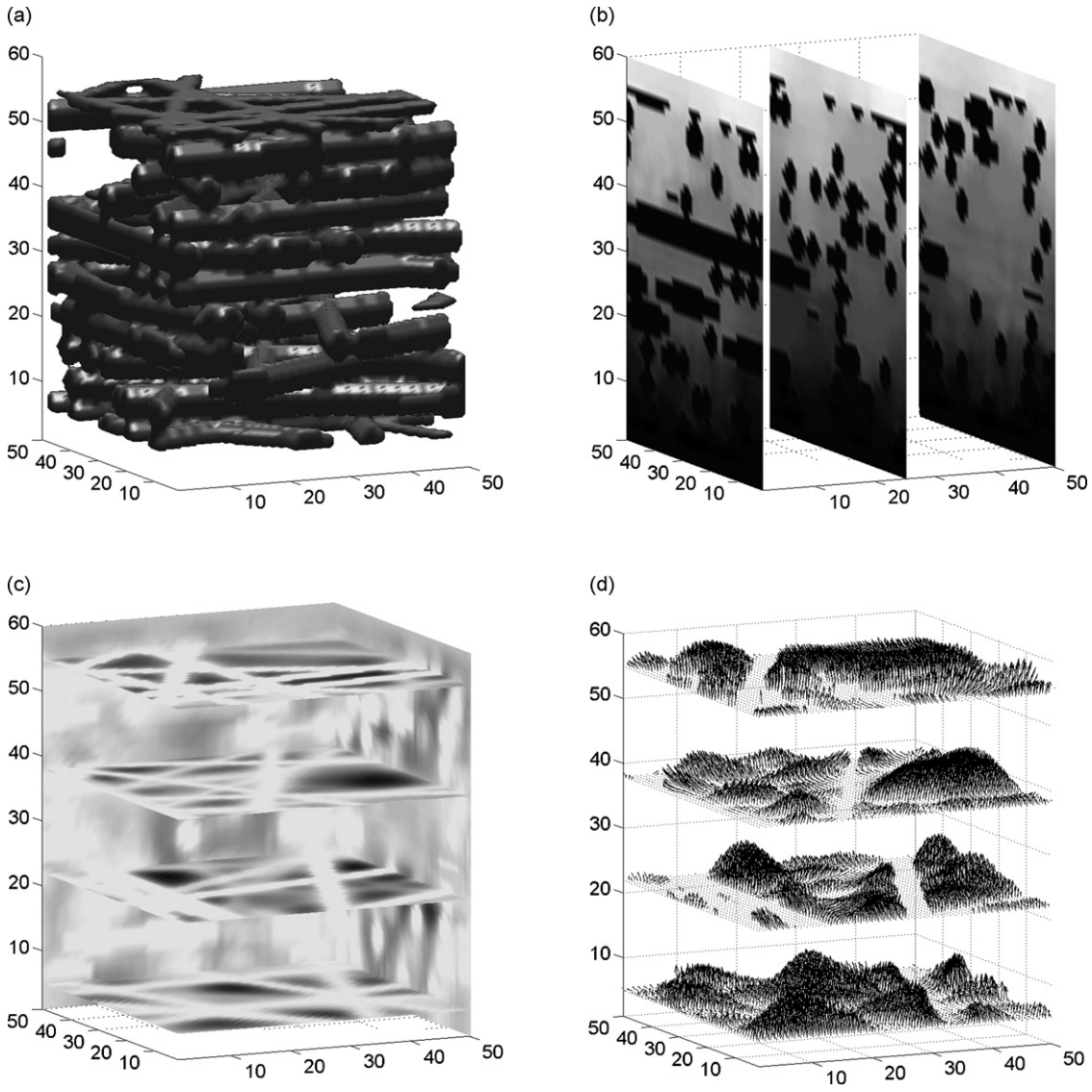

Fig. 12. Example of flow analysis results by LBM: (a) GDL structure, (b) pressure distribution, (c) flow rate distribution, and (d) velocity distribution.

determined by random numbers from an arbitrary vacant point. Walker does not move to solid phase. Walker moves m steps, and the distance r between the first position and the walker's position at step m is obtained. This process was tried n times, and the mean-square displacement $\langle r^2 \rangle$ was calculated as follows:

$$\langle r^2 \rangle = \frac{1}{n} \sum_{i=1}^{n} r_i^2 \tag{13}$$

Similarly, mean-square displacement in free space was calculated, and the tortuosity was obtained by dividing the value in free space by that in simulated GDL with various average porosities and diameters of fiber. As the assumption of a method of Watanabe and Nakashima [28] was that porous structure had isotropy, it should be noticed that the results of this calculation were not always equal to the actual tortuosity of GDL with anisotropy. Fig. 14 shows the relationship between porosity and tortuosity of simulated GDL, and it also shows the Tomadakis and Sotirchos model which is the model of fibrous porous media [27]. In this graph, it was found that calculation results of this study were almost equal to the value between in-plane and through-plane results of TS model. As the direction of diffusion was not determined in this calculation, these calculated values became intermediate value between both values of TS model. As a result, the validity of winding structure of this simulated GDL was confirmed qualitatively. In addition, there are some results which need to be focused on. Tortuosity ought to be independent of the diameter of fiber as long as geometrical similarity is kept. However, tortuosity was changed by the diameter of a fiber in this calculation. This result was caused by insufficiency of resolution, and it needs to be calculated with high resolution in the next study.

3.6. Evaluation of cell output performance with calculated tortuosity

PEFC cell output performance was evaluated by simple model including calculated tortuosity in simulated GDL. The

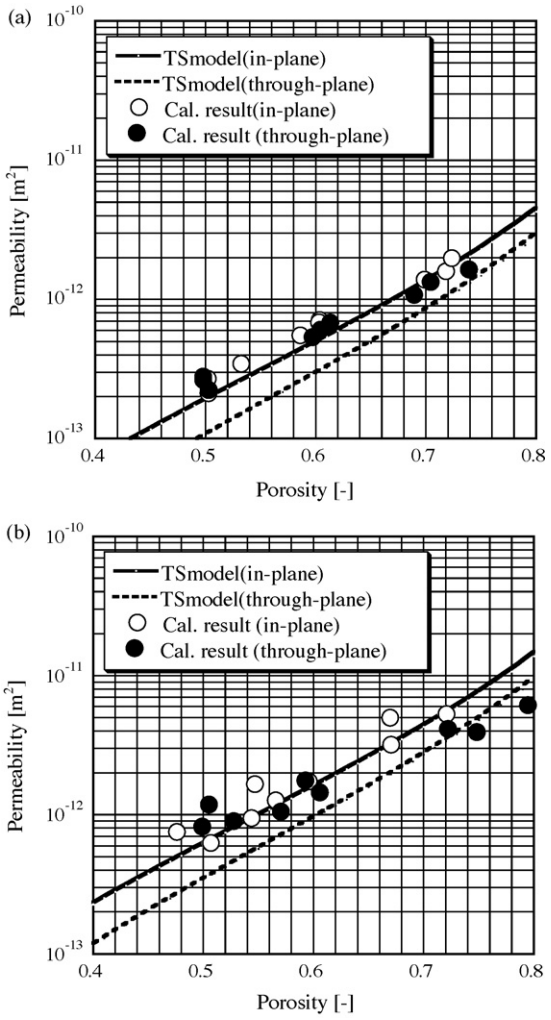

Fig. 13. Calculation results and TS model of relationship between in-plane and through-plane permeability and porosity with two sizes of fiber diameter: 5 μm (a), and 9 μm (b).

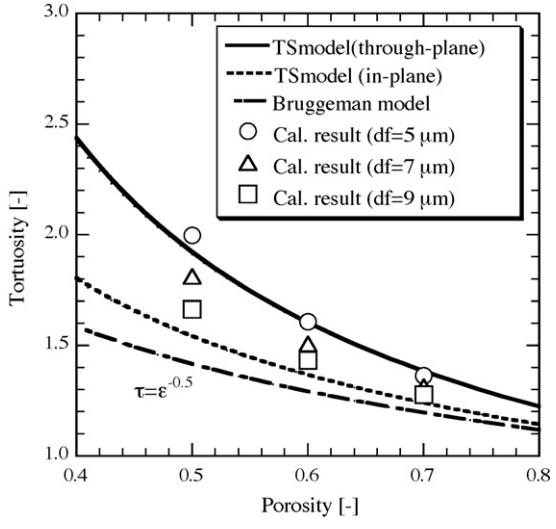

Fig. 14. Calculation results and TS model of relationship between tortuosity and porosity with various sized fiber diameter.

model equations were derived from our past model [12]. The oxygen diffusivity in cathode GDL was modeled, and the voltage was calculated by various overvoltage. In this study, it was assumed that there was only gas phase and that temperature was constant and uniform. In addition, the electrolyte membrane was humidified well, and ionic conductivity was constant and uniform. Though our past model included the gas flow through GDL, this flow was ignored in this study. The overvoltage of anode reaction was ignored, and the relationship between cell voltage and overvoltage is shown by the following equation:

$$V = E - \frac{RT}{\alpha_t 2F} \ln\left[\frac{iC_{O_2}^{ref}}{i_{O_2} C_{O_2}^{e}}\right] - R_{ohm} i \tag{14}$$

where E is the electromotive force, R the gas constant, T the temperature, α_t the transfer coefficient, F the Faraday's constant, i the current density, i_{O_2} the exchange current density, $C_{O_2}^{ref}$ the reference oxygen concentration, $C_{O_2}^{e}$ the oxygen concentration at an interface of catalyst layer and R_{ohm} is the resistance of proton transfer through the electrolyte membrane. R_{ohm} was calculated by Nguyen's equation [29]. Reference oxygen concentration and exchange current density were shown as the variable γ by the following equation:

$$\gamma = \frac{i_{O_2}}{C_{O_2}^{ref}} \tag{15}$$

The oxygen diffusion in GDL was simplified with the following equation which was derived from linear concentration gradient in Fick's law:

$$C_{O_2}^{e} = C_{O_2}^{channel} - \frac{i}{4F} \frac{L}{D_{O_2}} \frac{\tau}{\varepsilon} \tag{16}$$

where $C_{O_2}^{channel}$ is the oxygen concentration at a channel, L the thickness of GDL, D_{O_2} the oxygen diffusion coefficient, τ and ε are tortuosity and porosity in GDL. These tortuosity and porosity were obtained by the evaluation of simulated GDL in the previous section, and the effect of GDL structure on output performance was examined.

Calculation condition was shown in Table 3. However, as this model did not include the effect of liquid water, multi-content diffusion and heat transfer, it was not possible to compare the absolute values. So the maximum current density when porosity was 0.7 with simulated GDL was used as the reference value, and the output performance of each GDL was compared by using relative current density. Fig. 15 shows the current density–voltage curve of each GDL arranged by relative current density in the

Table 3
Calculation condition of output performance

Temperature (°C)	60
Transfer coefficient	0.3
Porosity	0.5–0.7
Electromotive force (V)	1.23
GDL thickness (μm)	200
Membrane thickness (μm)	30
Oxygen diffusion coefficient ($m^2\ s^{-1}$)	2.00×10^{-5}
γ of Eq. (15) ($A\ m\ mol^{-1}$)	4.0×10^{-2}

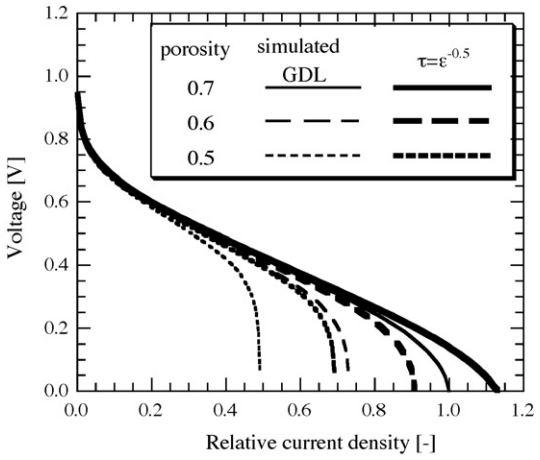

Fig. 15. Relative current density–voltage curve calculated from each tortuosity in the case of various porosities.

case of various porosities. Fine lines show the calculation results with tortuosity in simulated GDL in the case of 5 μm-diameter fiber, and bold lines show the Bruggeman equation. In this figure, it was found that the tortuosity affected to the output property, in particular, the influence was stronger in the case of low porosity. It was thought that the calculated results with Bruggeman equation which was generally used in other papers overestimate the diffusivity of GDL which consists of fibrous porous media. Moreover, though this model did not include the effect of liquid water, it is expected that it is important to know the substantial tortuosity relating the diffusivity in the case of two-phase condition. In this study, this model was so simple that the quantitative comparison could not be carried out. It will be needed to develop the high-accuracy model.

4. Conclusion

As a basic study for examination of flow and mass transfer in GDL with heterogeneous porous structure, the simulated GDL was developed by numerical analysis. The parameters were the diameter of a fiber, the average porosity and thickness. Furthermore, the structural properties, such as local porosity distribution, surface roughness, pore size distribution, permeability, tortuosity, were evaluated, and the validity was confirmed by comparing with the results of other studies. As a result, the effects of average porosity and the diameter of a fiber on these structural properties were clarified by numerical analysis. The prediction method of this study can be applied to other porous structure except for non-woven fabric, and it is thought that new GDL structure which contributes to the high power density and the high durability can be developed and proposed by this model. Moreover, optimal GDL structure can be examined by applying this method from the viewpoint of gas diffusivity and water discharging efficiency in GDL. Furthermore, the effective diffusion coefficient was calculated from tortuosity in simulated GDL, and PEFC output performance was evaluated with a simple model. It was confirmed that the diffusion overvoltage was largely affected by tortuosity on a general operating condition and that it was important to calculate the tortuosity with accuracy. However, as this evaluation of output performance did not include the effect of liquid water, multi-content diffusion and heat transfer, it will be needed to develop the model including these phenomena with simulated GDL in our future study. In addition, as GDL was transformed by clamp pressure, the influence of transformation will be considered. On the other hand, though pore diameter distribution was obtained as planate pore in this study, it is expected that pore size has three-dimensionality in a cubic structure. In our future study, it needs to be improved the prediction method of pore diameter distribution.

Acknowledgement

This research was supported by the research and development of polymer electrolyte fuel cell from the New Energy and Industrial Technology Development Organization (NEDO), Japan.

References

[1] D. Kramer, J. Zhang, R. Shimoi, E. Lehmann, A. Wokaun, K. Shinohara, G.G. Scherer, Electrochim. Acta 50 (2005) 2603–2614.
[2] J. Zhang, D. Kramer, R. Shimoi, Y. Ono, E. Lehmann, A. Wokaun, K. Shinohara, G.G. Scherer, Electrochim. Acta 51 (2006) 2715–2727.
[3] M. Hickner, N. Siegel, K. Chen, D. Hussey, D. Jacobson, M. Arif, Fuel Cell Seminar, Honolulu HI, November 13–17, 2006, pp. 380–383 (Abstracts).
[4] J. Ihonen, M. Mikkola, G. Lindbergh, J. Electrochem. Soc. 151 (2004) A1152–A1161.
[5] M.V. Williams, E. Begg, L. Bonville, H.R. Kunz, J.M. Fenton, J. Electrochem. Soc. 151 (2004) A1173–A1180.
[6] J.G. Pharoah, J. Power Sources 144 (2005) 77–82.
[7] U. Pasaogullari, C.Y. Wang, K.S. Chen, J. Electrochem. Soc. 152 (2005) A1574–A1582.
[8] U. Pasaogullari, C.Y. Wang, J. Electrochem. Soc. 151 (2004) A399–A406.
[9] G. Lin, W. He, T.V. Nguyen, J. Electrochem. Soc. 151 (2004) A1999–A2006.
[10] N.P. Siegel, M.W. Ellis, D.J. Nelson, M.R. von Spakovsky, J. Power Sources 128 (2004) 173–184.
[11] G. Inoue, Y. Matsukuma, M. Minemoto, J. Power Sources 154 (2006) 8–17.
[12] G. Inoue, Y. Matsukuma, M. Minemoto, J. Power Sources 157 (2006) 136–152.
[13] G. Inoue, Y. Matsukuma, M. Minemoto, J. Power Sources 157 (2006) 153–165.
[14] M.F. Mathias, J. Roth, J. Fleming, W. Lehnert, Handbook of Fuel Cells, vol. 3, Wiley, 2003, pp. 517–537 (Chapter 42).
[15] J.T. Gostick, M.W. Fowler, M.A. Ioannidis, M.D. Pritzker, Y.M. Volfkovich, A. Sakars, J. Power Sources 156 (2006) 375–387.
[16] H.K. Lee, J.H. Park, D.Y. Kim, T.H. Lee, J. Power Sources 131 (2004) 200–206.
[17] S. Succi, The Lattice Boltzmann Equation for Fluid Dynamics and Beyond, Oxford Science Publications, New York, 2001.
[18] D.A. Wolf-Gladrow, Lattice-Gas Cellular Automata and Lattice Boltzmann Models, Springer, New York, 2000.
[19] T. Yoshimoto, G. Inoue, Y. Matsukuma, M. Minemoto, Proceeding of Renewable Energy, Makuhari Japan, October 9–13, 2006, pp. 1364–1367.
[20] Y. Matsukuma, S. Sakashita, G. Inoue, M. Minemoto, Proceedings of the 15th Discrete Simulation of Fluid Dynamics (DSFD 2006) Conference, 2006.
[21] T. Koido, T. Furusawa, K. Moriyama, K. Takato, 210th Meeting of the Electrochemical Society, Cancun, Mexico, October 29–November 3, 2006.
[22] D.A. Nield, A. Bejan, Convection in Porous Media, Springer, New York, 1998.

[23] R.B. Bird, W. Steward, E.N. Lightfood, Transport Phenomena, Wiley, New York, 1960.
[24] J.T. Gostick, M.W. Fowler, M.D. Pritzker, M.A. Ioannidis, L.M. Behra, J. Power Sources 162 (2006) 228–238.
[25] M.M. Tomadakis, T.J. Robertson, J. Compos. Mater. 39 (2005) 163–188.
[26] J. van Brakel, P.M. Heertjes, Int. J. Heat Mass Transfer 17 (1974) 1093–1103.
[27] M.M. Tomadakis, S.V. Sotirchos, AIChE J. 39 (1993) 397–412.
[28] Y. Watanabe, Y. Nakashima, Comput. Geosci. 28 (2002) 583–586.
[29] T.V. Nguyen, R.E. White, J. Electrochem. Soc. 140 (1993) 2178–2186.